

# PCCP

Accepted Manuscript



This is an *Accepted Manuscript*, which has been through the Royal Society of Chemistry peer review process and has been accepted for publication.

*Accepted Manuscripts* are published online shortly after acceptance, before technical editing, formatting and proof reading. Using this free service, authors can make their results available to the community, in citable form, before we publish the edited article. We will replace this *Accepted Manuscript* with the edited and formatted *Advance Article* as soon as it is available.

You can find more information about *Accepted Manuscripts* in the [Information for Authors](#).

Please note that technical editing may introduce minor changes to the text and/or graphics, which may alter content. The journal's standard [Terms & Conditions](#) and the [Ethical guidelines](#) still apply. In no event shall the Royal Society of Chemistry be held responsible for any errors or omissions in this *Accepted Manuscript* or any consequences arising from the use of any information it contains.

## Dynamics of aqueous binary glass-formers confined in MCM-41

Khalid Elamin<sup>1</sup>, Helén Jansson<sup>2</sup> and Jan Swenson<sup>1</sup>

<sup>1</sup>Department of Applied Physics, Chalmers University of Technology, SE-412 96  
Göteborg, Sweden

<sup>2</sup>Department of Civil and Environmental Engineering, Chalmers University of  
Technology, SE-412 96 Göteborg, Sweden

### Abstract

Dielectric permittivity measurements were performed on water solutions of propylene glycol (PG) and propylene glycol monomethyl ether (PGME) confined in 21 Å pores of the silica matrix MCM-41 C10 in wide frequency ( $10^{-2}$ – $10^6$  Hz) and temperature (130–250 K) ranges. The aim was to elucidate how the formation of large hydrogen bonded structural entities, found in bulk solutions of PGME, was affected by the confined geometry, and to make comparisons with the dynamic behavior of the PG-water system. For all solutions the measurements revealed four almost concentration independent relaxation processes. The intensity of the fastest process is low compared to the other relaxation processes and might be caused by both hydroxyl groups of the pore surfaces and by local motions of water and solute molecules. The second fastest process contains contributions from both the main water relaxation as well as the intrinsic  $\beta$ -relaxation of the solute molecules. The third fastest process is the viscosity related  $\alpha$ -relaxation. Its concentration independency is very different compared to the findings for the corresponding bulk systems, particularly for the PGME-water system. The experimental data suggests that the surface interactions induce a micro-phase separation of the two liquids, resulting in a full molecular layer of water molecules coordinating to the hydrophilic hydroxyl groups on the surfaces of the silica pores. This, in turn, increases the geometrical confinement effect for the remaining solution

even more and prevents the building up of the same type of larger structural entities in the PGME-water system as in the corresponding bulk solutions. The slowest process is mainly hidden in the high conductivity contribution at low frequencies, but its temperature dependence can be extracted for the PGME-water system. However, its origin is not fully clear, as will be discussed.

## 1. Introduction

During the last several decades, the dynamics of molecular liquids in various confined geometries has been extensively studied,<sup>1-11</sup> due to their relevance in many technological and industrial processes, such as catalysis, chromatography or membrane separation.<sup>12</sup> In most of these studies, porous glasses with different pore dimensions have been used to obtain geometrically controlled confinements, and to help experimental physicists to evaluate models and concepts concerning the molecular dynamics in confined geometries. However, the effects of confinement have only begun to be understood, and often the experimental studies seem to give contradictory results.<sup>2,13</sup> The reason for the apparent contradictions is most likely that there is a competitive balance between confinement and surface effects, where geometrical confinements tend to speed-up,<sup>3,6,8,14-18</sup> and surface interactions normally lead to a slowing down of the dynamics<sup>1,19,20</sup>, respectively. However, this statement is not fully uncontroversial since some studies have suggested that also geometrical confinement effects can cause a slowing down of the dynamics.<sup>1,19,20</sup> Further complicating facts seem to be that the density of a liquid is often lower in a confined geometry, and that geometrical confinement effects are more dominating at low temperatures close to the glass transition. To resolve these issues different types of

liquids in different geometrical confinements, with various surface properties, have been studied to understand the confinement induced dynamical alterations.

In a confined geometry a liquid is expected to behave structurally and dynamically different at the surface-liquid interface than in the inner pore volume, where the molecules are less affected by surface interaction. Properties of the surface-liquid interface are governed predominantly by the polarities of the pore material and the liquid, which determine whether the liquid-surface interaction becomes attractive or repulsive. The behavior in the inner pore volume may depend on different factors, such as the type of intermolecular interactions (e.g. van der Waals or hydrogen bonding), size, mass and shape of the liquid molecules, density compared to bulk, cooperativity length of structurally rearranging regions, collective hydrodynamic effects, etc. This makes everything complicated and implies that the dynamics of surface molecules may be slowed down compared to bulk at the same time as the molecules in the inner pore region are moving faster than in bulk. For binary solutions, where the surface interactions can stimulate a micro-phase separation of the two confined liquids<sup>4,5,21,22</sup> the situation can be even more complex.

In the case of the here studied propylene glycol (PG) and propylene glycol monomethyl ether (PGME), these single liquids have previously been studied in various confined geometries by several different techniques, such as differential scanning calorimetry, broadband dielectric spectroscopy, neutron scattering and molecular dynamic simulations.<sup>1,11,13,19,24-33</sup> In most of these studies the dynamics of the liquids are altered compared to bulk and sometimes even new relaxation processes were observed.<sup>1</sup> The additional process in Ref. 1 was slower than the structural  $\alpha$ -

relaxation, and its intensity was about six orders of magnitude larger. The authors attributed this process to a surface layer of the liquid, whose rotational motion is strongly hindered by surface effects. In another study<sup>27</sup> of PG confined in droplets of butyl rubber two slower processes were observed in the frequency range below the structural  $\alpha$ -relaxation. The slowest process was assigned to be due to the liquid surface layer, while the faster one was believed to be caused by interfacial Maxwell–Wagner–Sillars polarization effects. However, Kremer *at al.*,<sup>13</sup> made an opposite interpretation in their study of low molecular weight glass-forming liquids confined in nanoporous sol-gel glasses and proposed a scenario the other way around, with the slowest process due to interfacial Maxwell–Wagner–Sillars polarizations and the faster one due to a surface layer.

The dynamic behavior of aqueous bulk solutions of propylene glycol (PG) and propylene glycol monomethyl ether (PGME) has been extensively studied by Sjöström *at al.*<sup>34,35</sup> In these studies, the strong influence of hydrogen bonds on the dynamics was evident; a PG molecule can hydrogen-bond to two other molecules, i.e. forming chains, whereas PGME has only one OH-group and can therefore only form molecular pairs. This difference in the ability of forming hydrogen bonds with other molecules gives rise to substantial differences in the glass transition related dynamical properties of PG and PGME.<sup>34</sup> For instance, the glass transition temperature ( $T_g$ ) of pure PG is around 168 K, and it decreases slightly with increasing water content up to 60 wt.% water, where partial crystallisation begin. In contrast, the  $T_g$  of PGME is around 143 K, and this value increases rapidly with increasing water content up to a concentration of 55 wt.%, and then decreases with even more water added. This non-monotonic behavior has been explained on the basis that the introduced water

molecules have a tendency to form bridges between two or more PGME molecules, and therefore larger structural entities are formed, which relax slower and, thus, give rise to an increase of  $T_g$ . The reason for a decreasing  $T_g$  at higher water contents is that the water molecules can no longer contribute to a further growth of the hydrogen bonded entities, which leads to a decrease of the glass transition temperature due to a common plasticizing effect of the additional water.<sup>35</sup>

In the present study, we have used broadband dielectric spectroscopy to study the relaxation dynamics of PG-water and PGME-water solutions confined in 21 Å pores of the silica matrix MCM-41 C10 in wide concentration, frequency ( $10^{-2}$ – $10^6$  Hz) and temperature (120 –250 K) ranges. The aim of this study was to elucidate how the confinement affects the glass transition related structural  $\alpha$ -relaxation, as well as the more local water relaxation of the solutions. Of particular interest is to determine whether the pronounced non-monotonic concentration dependence of the  $\alpha$ -relaxation of the PGME-water bulk solutions is maintained in the 21 Å pores. Thus, can the same type of larger relaxing entities be formed in the present confinement? Furthermore, the confined geometry prevents ice formation at all concentrations and temperatures and makes it possible to extend the investigation of the concentration dependent dynamics in the corresponding bulk solutions all the way to pure water.

The results show that the non-monotonic behavior of the structural  $\alpha$ -relaxation in bulk solutions of PGME is prevented in the present confinement. There are two reasons for this finding. Firstly, the strong confinement effect appears to reduce the ability of forming hydrogen bonded bridges of water molecules between PGME molecules, and, secondly, the surface interactions seem to induce a micro-phase

separation of the two liquids. Most likely, the water molecules have a stronger preference to coordinate to the hydroxyl surface groups of the silica pores, leaving most of the PG (or PGME) molecules in the centre of the pores, as previously indicated for aqueous solutions of glycerol<sup>4,5</sup> and 2PGME<sup>23</sup> confined in MCM-41.

## 2. Sample preparations and experimental details

The silica matrix MCM-41 C10 was prepared by the modified Beck method, as described in more detail in Ref.<sup>36</sup> A pore diameter of 21 Å was obtained by using long chain alkyltrimethylammonium bromide with 10 carbon atoms in the long alkyl group, i.e. C<sub>10</sub>H<sub>21</sub> (CH<sub>3</sub>)<sub>3</sub>N<sup>+</sup>Br, as the template organic reagent. The size of the pores was determined by N<sub>2</sub> adsorption at the temperature of liquid nitrogen, in which an analysis program developed by Dolimore-Heale was employed.<sup>37</sup> High-resolution electron microscopy was also employed to confirm the pore size, as described in Ref.<sup>37</sup>

The aqueous solutions (concentrations of 0, 20, 40, 60, 80 and 100 wt% water) were prepared by mixing propylene glycol (PG) of ≥ 99.5 % purity and propylene glycol monomethyl ether (PGME) of ≥ 98 % purity (purchased from Aldrich (C.A.S number are 57-55-6 and 107-98-2 respectively), with double distilled water (Milli-Q water). Prior to the sample preparation each solution was left in an ultrasonic bath for 30 min to ensure a homogenous mixing of the two liquids. Thereafter the PG-water and PGME-water solutions were confined in the 21 Å pores by soaking the vacuum dried MCM-41 C10 powder directly into the bulk solutions under vacuum. After the pores of MCM-41 C10 had been filled with the bulk solutions the powder was removed from the bulk solutions and gently dried by a tissue before the samples were measured

by broadband dielectric spectroscopy.

The dielectric measurements were performed on a broadband dielectric spectrometer from Novocontrol, equipped with a Novocontrol Alfa-S High Resolution Dielectric Analyser. The samples of the confined PG-water and PGME-water solutions were placed between two gold-plated brass electrodes of diameter 20 mm. The thickness of each sample was controlled to be 0.1 mm by using silica spacer fibres. Measurements were performed in the frequency and temperature ranges  $10^{-2}$ – $10^6$  Hz and 120–250 K, respectively. The temperature was controlled using a nitrogen gas cryostat, with temperature stabilization better than  $\pm 0.2$  K. Frequency scans were made at every fifth degree.

### 3. Results and Discussion

Fig. 1 shows the imaginary part of the permittivity ( $\epsilon''$ ), as a function of frequency, of the confined solution of PG-water containing 40 wt% water, at some selected temperatures in the range 160–240 K. In this temperature range three relaxation processes can be observed; the viscosity related structural  $\alpha$ -relaxation and two faster and more local processes, which here are denoted the  $w$ -relaxation and the fast process, see Fig. 1. The two latter relaxation processes are most easily observed at low temperatures below 180 K, where they are considerably faster than the  $\alpha$ -relaxation. However, the intensity of the fastest process is weak compared to the  $\alpha$ - and the  $w$ -relaxations, which made it difficult to determine its temperature dependence. In this case, its concentration independence helped us to establish its Arrhenius temperature dependence, as shown below. The physical origin of this fast

process cannot be fully determined, but it can be caused by both hydroxyl groups<sup>38</sup> and/or by local motions of water and solute molecules. However, even if a similar process is commonly observed for water in a wide range of materials,<sup>39</sup> it should be noted that it is here also observed for the sample without water, which favours the assignment to the hydroxyl groups. Somewhat above 170 K this process seems to merge with the  $w$ -relaxation. This  $w$ -relaxation is commonly observed for water in hard confinements,<sup>38,40,41</sup> where it shows a nearly universal behavior. Also in aqueous bulk solutions a similar  $w$ -relaxation can be observed below  $T_g$ .<sup>34,41-45</sup> With increasing temperature a third process enters into the experimental frequency window from the low frequency side. This is the  $\alpha$ -relaxation and in Fig. 1 it can be observed that the temperature dependence of this relaxation is much stronger than that for the  $w$ -relaxation (and the fastest process at low temperatures). Therefore, these processes approach each other and above 190 K they can no longer be distinguished.

At relatively high temperatures also conductivity and polarization effects are giving strong contributions in the low frequency region. In fact, this so-called low frequency dispersion obscures another, even slower, process to be clearly observed in the raw data of the PG-water solutions. However, after subtraction of the conductivity contribution from the raw data it is possible to establish its presence. From Fig. 2 it is obvious that a similar process exists also in the PGME-water solutions. In this case it can be observed without any subtraction since it is displayed by a weak shoulder in the conductivity. The reason for why this slow process is more easily observed for the PGME-water system is likely that the neighboring  $\alpha$ -relaxation in this system is much weaker than in the PG-water system, as shown below. The origin of, this process is not fully clear, as will be further discussed below.

Fig. 2 also shows the concentration dependences of the  $w$ -relaxation, the main structural  $\alpha$ -relaxation and the slowest relaxation process in the confined solutions of PGME-water at  $T=185$  K. From this figure, it is obvious that the  $w$ -relaxation is observed for all water concentrations, i.e. also for the sample without water as well as for confined water, as shown in Refs. 38 and 40. This implies that it must contain contributions from both the intrinsic  $\beta$ -relaxation of confined PGME (or PG) as well as from a water relaxation. In fact, these two relaxation processes seem to occur at almost exactly the same frequency. Similar findings were also obtained for glycerol-water solutions in the same confinement.<sup>4</sup> It should also be noted that at lower temperatures a faster relaxation process was observed, similar to what we observed for the confined PG-water solutions. However, since this local process is even weaker in this system, at least compared to the neighboring  $w$ -relaxation, its temperature dependence is difficult to determine with certainty, although it appears to exhibit a similar Arrhenius behavior as for the confined PG-water solutions.

For a more quantitative determination of how the relaxation processes change with temperature and water concentration we have curve fitted the dielectric loss data shown in Figs. 1 and 2. Examples of such curve fitted data are presented in Fig. 3(a) and (b) for the confined solutions of PG-water and PGME-water, containing 40 wt% water, at  $T=185$  K. These systems are, as described above, very complex and therefore five standard fit functions were needed to describe their spectra (however, not necessarily all of them at a given temperature): a power law for the conductivity contribution, a Havriliak-Negami function<sup>46</sup> for the  $\alpha$ -relaxation and three symmetric

Cole-Cole functions<sup>47</sup> for the slow process,  $w$ -relaxation and the fastest process. Thus, for each sample the total fit function was given by:

$$\varepsilon''(\omega) = \frac{\sigma}{i\varepsilon_0\omega} + \frac{\Delta\varepsilon_s}{1+(i\omega\tau_s)^a} + \frac{\Delta\varepsilon_\alpha}{(1+(i\omega\tau_\alpha)^a)^b} + \frac{\Delta\varepsilon_w}{1+(i\omega\tau_w)^a} + \frac{\Delta\varepsilon_f}{1+(i\omega\tau_f)^a} \quad (1)$$

where  $\omega$  is the angular frequency,  $\sigma$  is the dc conductivity,  $\tau_s$ ,  $\tau_\alpha$ ,  $\tau_w$  and  $\tau_f$  are the relaxation times for the slow,  $\alpha$ ,  $w$  and fast relaxation, respectively,  $\Delta\varepsilon_s$ ,  $\Delta\varepsilon_\alpha$ ,  $\Delta\varepsilon_w$  and  $\Delta\varepsilon_f$  are the dielectric strengths of the same processes, and  $a$  and  $b$  are the shape parameters that determine the symmetric and asymmetric broadening of the relaxation peaks, respectively. The shape parameters obtained from this fitting procedure are presented in Tables 1 and 2 as average values for the temperature ranges the processes could be observed, and with the temperature variations as “error bars”. From these tables it is evident that these shape parameters are only weakly dependent on the water concentration. The major difference is observed in the case of the shape parameter  $a$  for the  $\alpha$ -relaxation, which has a considerably smaller value (i.e. the symmetric broadening is larger) for the confined PGME solutions than for the confined PG solutions. The  $w$ -relaxation is also slightly broader (the shape parameter  $a$  has a lower value) in the case of the PG solutions. The concentration dependence of the ratio between  $\Delta\varepsilon_\alpha$  and  $\Delta\varepsilon_w$  is also interesting and therefore shown in Fig. 4 for the same solutions and at the same temperature as shown in Fig. 3. From this figure it is clear that the relative intensity of the structural  $\alpha$ -relaxation, compared to the intensity of the  $w$ -relaxation, is much weaker for the PGME-water system than for the PG-water solutions. In fact, for the confined PGME-water solutions the  $\alpha$ -relaxation is even weaker (or about the same), as the  $w$ -relaxation. Since the intensity of the  $w$ -relaxation is expected to be relatively similar in the two systems (at least at higher

water concentrations where its main contribution comes from the water), this finding suggests that the  $\alpha$ -relaxation is weaker in the PGME solutions than in the PG solutions. Although one should be careful to draw conclusions from absolute intensities it is clear from Fig. 3 that this indication is supported by the much higher absolute intensity of the  $\alpha$ -relaxation in the confined PG-water solution. Generally, the cooperative, and more large-scale, motions in solutions are more suppressed by confinements than the more local relaxation processes. This has, for instance, been observed for these solutions<sup>48</sup> and other molecular glass-formers<sup>26</sup> confined in a two-dimensional layer-structured Na-vermiculite clay. However, in our case this enhanced confinement effect on the  $\alpha$ -relaxation is less pronounced. Other somewhat unexpected findings from Figs. 2 and 4, are the weak concentration dependence of the peak position of the  $\alpha$ -relaxation (further discussed below) and the non-monotonic concentration dependence of its intensity, with a maximum at an intermediate water concentration. Since previous studies of confined solutions<sup>5</sup> have shown that the intensity of the  $\alpha$ -relaxation tends to decrease with increasing water content (note here that no  $\alpha$ -relaxation can be observed for confined water) a similar behaviour had been expected also for the solutions of PG and PGME. The physical reason for why this is not observed is not fully clear, but maybe the length-scale of the cooperativity of the  $\alpha$ -relaxation does not only increase when pure water is approached,<sup>5</sup> but also when the water content approaches zero. Another plausible explanation is that a lower amount of the liquid/solution fills the pores at high PGME contents. This should also suppress the relative intensity of the  $\alpha$ -relaxation and produce a non-monotonic concentration dependence when it is combined with the known trend<sup>5</sup> of a decreasing intensity with increasing water content.

By using Eq. (1) to describe the experimental data we were able to determine the temperature dependent relaxation times of the slow,  $\alpha$ ,  $w$  and the fast relaxations, as shown in Fig. 5(a) and (b) for the confined solutions of PG-water and PGME-water, respectively. As mentioned above, at high temperatures also a process slower than the  $\alpha$ -relaxation could be observed for confined solutions of PG-water, but due to the high conductivity contribution at low frequencies (that to a large extent mask this process), its temperature development is difficult to establish with certainty. Therefore, the temperature dependence of this process is not presented in Fig. 5(a).

From Fig. 5 it is clear that the slow,  $\alpha$ ,  $w$  and fast relaxations in the confined solutions of PG-water (a) and PGME-water (b) can be distinguished by their temperature dependences. The viscosity related structural  $\alpha$ -relaxation of both systems and the slow relaxation process for PGME-water show a non-Arrhenius type temperature dependence that is well described by the Vogel-Fulcher-Tammann (VFT) function<sup>49-51</sup>:

$$\tau_{\alpha} = \tau_0 \exp\left(\frac{DT_0}{T-T_0}\right) \quad (2)$$

where  $\tau_0$  is the relaxation time extrapolated to infinite temperature and  $T_0$  is the temperature where the relaxation time  $\tau_{\alpha}$  extrapolates to infinity. The parameter  $D$  determines the deviation from Arrhenius temperature dependence, and it is related to the fragility of the glass forming liquid. The values of the fit parameters are given in Table 1, where the small differences between the samples of different water concentrations are equally evident as in Fig. 5. From these VFT-fits it is possible to

estimate the temperatures where these relaxation processes reach a time scale of 100 s,  $T_{100s}$ . For the  $\alpha$ -relaxation this temperature is often in agreement with the calorimetric  $T_g$  and therefore is considered as a dielectric glass transition temperature. The so obtained values of  $T_{100s}$  are also shown in Table 1.

The  $w$  and the fast relaxation are secondary ( $\beta$ ) and more local processes and are therefore only observed in the glassy and deeply supercooled regimes, where the  $w$ -relaxation is decoupled from the structural  $\alpha$ -relaxation, as shown in Fig. 5. The temperature dependence of the  $w$  and the fast relaxation, is given by the Arrhenius equation below  $T_g$ :

$$\tau_\beta = \tau_0 \exp\left(\frac{E_a}{k_B T}\right) \quad (3)$$

where  $E_a$  is the activation energy of the relaxation process. Values of the fit parameters  $\tau_0$  and  $E_a$  for these two relaxation processes are provided in Table 2. From the values it is evident that also these relaxation processes are only weakly dependent on the water concentration, and also similar for the confined solutions of PG and PGME.

In Fig. 5 it should be noted that the temperature dependence of the  $w$ -relaxation time deviates from its low temperature Arrhenius behaviour above  $T_g$ . To determine whether this is a real effect or due to the simplification that the  $\alpha$  and  $w$  relaxations have been treated as independent processes, i.e. the two processes are additively combined in Eq. 1, we also used Williams-Watts ansatz<sup>52</sup> to fit the dielectric loss data around  $T_g$ . Since a substantial fraction of the liquid molecules should participate in

both relaxation processes this approach should be more correct. However, this analysis changed the relaxation times of the  $\alpha$  and  $w$  processes only slightly, and the deviation of  $\tau_w$  from its low temperature Arrhenius behaviour remained. This indicates that the change of its activation energy around  $T_g$  is real and caused by a change in its relaxation mechanism at  $T_g$ .<sup>53</sup>

It is also interesting to note that the concentration dependence of  $\tau_w$  is very weak, as shown in Fig. 5. This implies that the water relaxation must have similar temperature dependence as the intrinsic  $\beta$ -relaxation of confined PG and PGME. This indicates that both the water and the solute molecules are moving locally on a similar time scale and with the same activation energy, leading to that only a combined  $w$ -relaxation is observed.

As discussed above, also the structural  $\alpha$ -relaxation is almost concentration independent, and this behavior is in strong contrast to not only the corresponding bulk solutions, particularly the solutions of PGME,<sup>34</sup> but also to what was observed for the same solutions confined in the quasi-two-dimensional interlayer space of clay.<sup>48</sup> In the clay confinement the calorimetric  $T_g$  of the PGME-water system was found to exhibit a similar non-monotonic concentration dependence as for the corresponding bulk system, even if the associated  $\alpha$ -relaxation could not be directly observed at higher water contents.<sup>48</sup> In the present case the lack of a non-monotonic concentration dependence of the  $\alpha$ -relaxation time indicates that the growth of larger relaxing structural entities is suppressed in the 21 Å pores of the MCM-41. Hence, in this system the water molecules are probably not able to form hydrogen bonded bridges between different PGME molecules. This finding is also in contrast to a recent

quasielastic neutron scattering (QENS) study on di-PGME-water solutions confined in 28 Å pores of MCM-41,<sup>23</sup> which showed that larger structural entities of two di-PGME molecules and bridging water molecules were formed, as in the corresponding bulk solutions, but only at considerably higher water contents. The reason for this shift to higher water concentrations is most likely that the water molecules have a stronger preference to coordinate to the hydroxyl surface groups of the silica pores, leaving most of the solute molecules in the centre of the pores. Such a micro-phase separation of the two liquids has also been indicated to occur for aqueous solutions of glycerol<sup>4,5</sup> confined in the same MCM-41 as used in this study. Thus, also for the present PG-water and PGME-water solutions the water molecules are expected to have a stronger preference to coordinate to the hydroxyl surface groups of the silica pores than the solute molecules. A surface layer of water molecules would also reduce the effective pore size for the solution with 6-7 Å, leading to an available pore size of only 13-14 Å for the formation of hydrogen bonded larger structural entities. Since this pore size seems to be too small for such structural formations, but sufficient for 28 Å pores reduced by 6-7 Å for the water layer, the required size for the formation of the same hydrogen bonded larger entities as in bulk solutions of PGME should be between 14 Å and 21 Å.

In Fig. 6 comparisons between some of the confined and bulk solutions of PG-water and PGME-water, respectively, are shown for the relaxation times of the  $\alpha$  and  $w$  processes. Fig. 6(c) shows that the  $\alpha$ -relaxation time of the confined solutions of PG-water is identical to the  $\alpha$ -relaxation time of bulk PG. Thus, the common plasticizing effect of water and the associated speeding up of the  $\alpha$ -relaxation (and reduction in  $T_g$  as shown in Fig. 6(a)), as observed for the bulk system of PG-water, cannot be

observed for the confined solutions of PG-water. This suggests that the PG molecules are moving independently of the water molecules, which further supports that the two liquids are micro-phase separated in the silica pores. Although the  $\alpha$ -relaxation of confined PGME is substantially slower than for bulk PGME, see Fig. 6(d), its insensitivity to added water suggests that also PGME and water are partially micro-phase separated, as in the case of the aqueous solutions of di-PGME in the larger pore size of 28 Å.<sup>23</sup> However, at 60 and 80 wt% water there is a clear indication of that water participates in the  $\alpha$ -relaxation, since a crossover to an Arrhenius temperature dependence occurs before the time scale of the glass transition (i.e. a relaxation time of about 100 s) is reached, see the change from solid to open symbols of the  $\alpha$ -relaxation in Fig. 5(b). Such a decoupling of local water dynamics from the  $\alpha$ -relaxation of an aqueous solution is commonly observed to occur close to  $T_g$ .<sup>39,54-59</sup> In this case the activation energy of the decoupled water relaxation is higher than the faster and more “universal” water relaxation, i.e. the  $w$ -relaxation, and the decoupling occurs at a slow relaxation time of about 10 ms. Its high activation energy and “late” decoupling from the  $\alpha$ -relaxation indicates, by comparing with other aqueous solutions as well as the corresponding bulk solutions,<sup>34</sup> that only a relatively low weight fraction of water is involved in the  $\alpha$ -relaxation of these water concentrations of 60 and 80 wt%. Thus, also this finding suggests that the confined PGME-water solutions are partially micro-phase separated with a full molecular layer of water molecules coordinating to the hydrophilic hydroxyl groups on the surfaces of the silica pores. This, further implies that the lack of a non-monotonic concentration dependence of the  $\alpha$ -relaxation, and its associated  $T_g$  shown in the inset of Fig. 6(b), of the PGME-water solutions can be explained by a combination of this partial micro-phase separation and geometrical confinement effects, which obstruct the growth of

larger relaxing structural entities, as discussed above. In the near future, the structure of this system will be explored in more detail by neutron diffraction measurements and structural modelling.

From Fig. 6(e) and (f) it is also clear that the  $w$ -relaxation of the confined solutions has basically the same activation energy as in the corresponding bulk solutions. However, an important difference is that the time scale of this process is almost independent of the water concentration in the case of the confined solutions, whereas it becomes considerably faster with increasing water content (at least up to 50-60 wt% water) in the corresponding bulk solutions.<sup>34</sup> This observation is another indication of that the two liquids become essentially micro-phase separated in the silica pores (up to intermediate water concentrations), and therefore the water behaves as supercooled water in hard confinements (which commonly shows a “universal” relaxation behavior), rather than as supercooled water in solutions (which speeds up with increasing water content). For a more detailed discussion about the difference in the relaxation behavior of water in hard confinements and solutions we refer to a previous publication.<sup>41</sup>

Finally, we discuss the nature of slowest relaxation process, which was most clearly observed for the confined PGME-water solutions. The actual origin of this process is not clear and cannot be established from the present results, but in principle two scenarios exist. One scenario is that this process is due to interfacial polarization, i.e. the so-called Maxwell-Wagner-Sillars polarization, which generally occurs at a longer time scale than the  $\alpha$ -relaxation in powders and other inhomogeneous systems like the here investigated confined liquids.<sup>13,27,40</sup> In addition, such a process is commonly

characterized by a huge amplitude compared to the  $\alpha$ -relaxation, and a narrow symmetric shape with a broadening close to Debye. However, as obvious from Figs. 2 and 3(b) and the shape parameter  $a$  in Table 1, the intensity and shape of the slowest process is far from that expected for a Maxwell-Wagner-Sillars polarization process. In fact, its features are similar to a structural  $\alpha$ -relaxation, although with an atypical symmetric broadening. It should however be noted that the shape of this slow process is difficult to determine due to that it is partly hidden by the strong conductivity contribution at low frequencies. Keeping in mind the micro-phase separation inside the pores, it is not possible to rule out that also this slowest process has the nature of a  $\alpha$ -relaxation. Such an interpretation is also supported by the observation that  $\tau_w$  deviates from its low temperature Arrhenius dependence when this process reaches a time scale of 100 s, i.e. the dielectric  $T_g$ . This expected relation is even better for this process than for the somewhat faster process that we have denoted as the  $\alpha$ -relaxation, since it shows the characteristics of a typical  $\alpha$ -relaxation. The problem with the interpretation that the micro-phase separation gives rise to two  $\alpha$ -relaxations is, however, that the slow process is observed also in PGME, without any water. Therefore, all kind of interpretations are complicated, and consequently it is difficult to establish its origin. However, it is important to note that the main conclusions of this paper are valid irrespective whether this process is due to interfacial polarization effects or has the nature of a  $\alpha$ -relaxation, since also this process is almost concentration independent with similar temperature dependence as the process we have denoted as the  $\alpha$ -relaxation. It only occurs on a slower time scale.

#### 4. Conclusions

We have presented results from dielectric relaxation studies of aqueous solutions of propylene glycol (PG) and propylene glycol monomethyl ether (PGME) confined in 21 Å pores of the silica matrix MCM-41 C10. Four relaxation processes could be observed for both systems at all water contents, which is in contrast to confined water, where only one relaxation process was clearly observed in the measured temperature range. The viscosity related  $\alpha$ -relaxation shows an almost concentration independent non-Arrhenius temperature dependence, which is very different compared to the corresponding bulk systems. It can be explained by two major alterations occurring in the confinement. Firstly, no larger structural entities of PGME molecules and bridging water molecules are formed in the present confinement and, secondly, there are clear indications for both systems that the two components in the solutions are not properly mixed in the silica pores. The water molecules seem to have a stronger preference to coordinate to the hydroxyl surface groups of the silica pores, resulting in a partial micro-phase separation of the two components and a partial mixing only at higher water concentrations. A partial mixing at higher water concentrations is at least evident for the confined PGME-water system, since a decoupling of a water relaxation from the cooperative  $\alpha$ -relaxation was observed close to  $T_g$ , as typical for aqueous bulk solutions. Thus, in this system some water should be located in the PGME-rich phase at high water contents. This further implies that the partial micro-phase separation cannot be the only reason for that no larger relaxing structural entities are formed in the confinements. The geometrical confinement effect must also prevent larger structural entities of hydrogen bonded molecules to be formed at higher water concentrations. Hence, the findings suggest that the 21 Å pores, where 6-7 Å

are devoted to the surface layer of water molecules, are too small for the formation of the same type of larger relaxing structural entities as observed in the corresponding bulk solutions. Finally, we note that the main water relaxation shows a similar temperature dependence as the intrinsic  $\beta$ -relaxation of the solute, even at high water contents, and therefore the two processes cannot be distinguished from each other.

### **Acknowledgements**

We are thankful to Shigeharu Kittaka for making and providing the MCM-41. This work was financially supported by the Swedish Research Council and the Swedish Energy Agency.

**References**

- 1 J. Schüller, Y. B. Melnichenko, R. Richert and E. W. Fischer, *Phys. Rev. Lett.*, 1994, **73**, 2224.
- 2 M. Arndt, R. Stannarius, H. Grootjens E. Hempel and F. Kremer, *Phys. Rev. Lett.*, 1997, **79**, 2077.
- 3 A. Schönhals and R. Stauga, *J. Chem. Phys.*, 1998, **108**, 5130.
- 4 K. Elamin, H. Jansson, S. Kittaka and J. Swenson, *Phys. Chem. Chem. Phys.*, 2013, **15**, 18437.
- 5 J. Swenson, K. Elamin, H. Jansson and S. Kittaka, *Chem. Phys.*, 2013, **424**, 20.
- 6 A. Schönhals and R. Stauga, *J. Non-Cryst. Solids*, 1998, **235–237**, 450.
- 7 A. Schönhals, H. Goering and Ch. Schick, *J. Non-Cryst. Solids*, 2002, **140 – 149**, 305.
- 8 A. Huwe, F. Kremer, P. Behrens et al., *Phys. Rev. Lett.*, 1999, **82**, 2338.
- 9 S. H. Anastasiadis, K. Karatasos, G. Vlachos et al., *Phys. Rev. Lett.*, 2000, **84**, 915.
- 10 R. Bergman and J. Swenson, *Nature (London)*, 2000, **403**, 283.
- 11 J. Swenson and W. S. Howells, *J. Chem. Phys.*, 2002, **117**, 857.
- 12 P. Scheidler, W. Kob, K. Binder, *Eur. Phys. J. E*, 2003, **12**, 5.
- 13 M. Arndt, R. Stannarius, W. Gorbatschow and F. Kremer, *Phys. Rev. E*, 1996, **54**, 5377.
- 14 G. Barut, P. Pissis, R. Pelster, and G. Nimtz, *Phys. Rev. Lett.*, 1998, **80**, 3543.
- 15 J. Baschnagel, C. Mischler, and K. Binder, *J. Phys. IV*, 2000, **10**, 9.
- 16 A. Huwe, F. Kremer, L. Hartmann et al., *J. Phys. IV*, 2000, **10**, 59.
- 17 A. Schönhals, H. Goering, Ch. Schick, B. Frick, and R. Zorn, *Eur. Phys. J. E*, 2003, **12**, 173.

- 18 C. Alba-Simionesco, G. Dosseh, E. Dumont, B. Frick, B. Geil, D. Morineau, V. Teboul, and Y. Xia, *Eur. Phys. J. E*, 2003, **12**, 19.
- 19 Y. B. Melnichenko, J. Schuller, R. Richert, B. Ewen, and C. K. Loong, *J. Chem. Phys.*, 1995, **103**, 2016.
- 20 R. Yamamoto and K. Kim, *J. Phys. IV*, 2000, **10**, 15.
- 21 A. Lerbret, G. Lelong, P. E. Mason, M.-L. Saboungi and J. W. Brady, *J. Phys. Chem. B*, 2011, **115**, 910.
- 22 X.-Y. Guo, T. Watermann and D. Sebastiani, *J. Phys. Chem. B*, 2014, **118**, 10207.
- 23 J. Swenson, K. Elamin, G. Chen, W. Lohstroh and V. Garcia Sakai, *J. Chem. Phys.*, 2014, **141**, 214501..
- 24 S. Cervený, J. Mattsson, J. Swenson and R. Bergman, *J. Phys. Chem. B*, 2004, **108**, 11596.
- 25 J. Swenson, G. A. Schwartz, R. Bergman and W.S. Howells, *Eur. Phys. J. E*, 2003, **12**, 179.
- 26 R. Bergman, J. Mattsson, C. Svanberg, G. A. Schwartz and J. Swenson, *Eur. Phys. Lett.*, 2003, **64**, 675.
- 27 P. Pissis, A. Kyritsis, D. Daoukaki, G. Barut, R. Pelster and G. Nimtz, *J. Phys.: Condens. Matter*, 1998, **10**, 6205.
- 28 W. Gorbatschow, M. Arndt, R. Stannarius and F. Kremer, *Eur. Phys. Lett.*, 1996, **35**, 719.
- 29 J. Swenson, D. Engberg, W. S. Howells, T. Seydel and F. Juranyi, *J. Chem. Phys.*, 2005, **122**, 244702.
- 30 T. R. Prisk, M. Tyagi and P. E. Sokol, *J. Chem. Phys.*, 2011, **134**, 114506.
- 31 V. Crupi, A. J. Dianoux, F. Longo, D. Majolino, P. Migliardo, V. Venuti, *J. Molec. Struct.*, 2005, **744–747**, 797.

- 32 K. Górny, Z. Dendzik, P. Raczynski, Z. Gburski, *Solid State Communications*, 2012, **152**, 8.
- 33 Z. Dendzik, K. Górny, W. Gwizdala, Z. Gburski, *J. Non-Cryst. Solids*, 2011, **357**, 575.
- 34 J. Sjöström, J. Mattsson, R. Bergman, E. Johansson, K. Josefsson, D. Svantesson and J. Swenson, *Phys. Chem. Chem. Phys.*, 2010, **12**, 10452.
- 35 J. Sjöström, J. Mattsson, R. Bergman and J. Swenson, *J. Phys. Chem. B*, 2011, **115**, 10013.
- 36 T. Mori, Y. Kuroda, Y. Yoshikawa, M. Nagao and S. Kittaka, *Langmuir*, 2002, **18**, 1595.
- 37 S. Kittaka, S. Ishimaru, M. Kuranishi, T. Matsuda and T. Yamaguchi, *Phys. Chem. Chem. Phys.*, 2006, **8**, 3223.
- 38 J. Hedström, J. Swenson, R. Bergman, H. Jansson and S. Kittaka, *Eur. Phys. J. Spec. Top.*, 2007, **141**, 53
- 39 J. Swenson, H. Jansson, J. Hedström and R. Bergman, *J. Phys.: Condens. Matter*, 2007, **19**, 205109.
- 40 J. Sjöström, J. Swenson, R. Bergman and S. Kittaka, *J. Chem. Phys.*, 2008, **128**, 154503.
- 41 J. Swenson and S. Cerveny, *J. Phys.: Condens. Matter*, 2015, **27**, 033102.
- 42 S. Cerveny, G. Schwartz, A. Alegria, R. Bergman and J. Swenson, *J. Chem. Phys.*, 2006, **124**, 194501.
- 43 N. Shinyashiki, S. Sudo, S. Yagihara, A. Spanoudaki, A. Kyritsis and P. Pissis, *J. Phys.: Condens. Matter*, 2007, **19**, 205113.
- 44 S. Cerveny, J. Colmenero and A. Alegria, *J. Non-Cryst. Solids*, 2007, **353**, 4523.
- 45 S. Cerveny, A. Alegria and J. Colmenero, *Phys. Rev. E*, 2008, **77**, 031803.

- 46 S. Havriliak and S. Negami, *Polymer*, 1967, **8**, 161.
- 47 K. S. Cole and R. H. Cole, *J. Chem. Phys.*, 1941, **9**, 341.
- 48 K. Elamin, J. Björklund, F. Nyhlén, M. Yttergren, L. Mårtensson and J. Swenson, *J. Chem. Phys.*, 2014, **141**, 034505.
- 49 H. Vogel, *Phys. Z.*, 1921, **22**, 645.
- 50 G. S. Fulcher, *J. Am. Ceram. Soc.*, 1925, **8**, 339.
- 51 G. Tammann and W. Hesse, *Z. Anorg. Allg. Chem.*, 1926, **156**, 245.
- 52 G. Williams, *Adv. Polym. Sci.*, 1979, **33**, 60.
- 53 K. L. Ngai and S. Capaccioli, *Phys. Rev. E*, 2004, **69**, 031501.
- 54 K. L. Ngai, S. Capaccioli and N. Shinyashiki, *J. Phys. Chem. B*, 2008, **112**, 3826.
- 55 H. Jansson, R. Bergman and J. Swenson, *J. Phys. Chem. B*, 2011, **115**, 4099.
- 56 M. Tarek and D. Tobias, *Phys. Rev. Lett.*, 2002, **88**, 138101.
- 57 J. Swenson, H. Jansson and R. Bergman, *Phys. Rev. Lett.*, 2006, **96**, 247802.
- 58 S. Cervený, G. A. Schwartz, R. Bergman and J. Swenson, *Phys. Rev. Lett.*, 2004, **93**, 245702.
- 59 N. Shinyashiki, W. Yamamoto, A. Yokoyama, T. Yoshinari, S. Yagihara, R. Kita, K. L. Ngai and S. Capaccioli, *J. Phys. Chem. B*, 2009, **113**, 14448.

### Figure Captions

Fig. 1. Imaginary part of the permittivity as a function of frequency of the confined solution of PG-water containing 40 wt.% water, at some selected temperatures from 160 K to 240 K.

Fig. 2. Imaginary part of the permittivity as a function of frequency of confined solutions of PGME-water of different water contents, at  $T=185\text{K}$ . The weight fraction of water in each sample is given in the figure.

Fig. 3. Frequency dependence of the imaginary part of the permittivity at  $T=185\text{ K}$  for the confined solutions of PG-water and PGME-water, containing 40 wt% water, are shown in (a) and (b), respectively. The solid line is the total fit to the experimental data, using Eq. 1. At this temperature the measured data are well described by a power law for the dc-conductivity, a Havriliak-Negami function for the  $\alpha$ -relaxation and two Cole-Cole functions for the  $w$ -relaxation and the fastest process of the confined solution of PG-water shown in (a). The same fit functions were used to describe the spectra of the confined solution of PGME-water shown in (b), the only difference is that the Cole-Cole function used to fit the fastest process now is used to fit the slowest process.

Fig. 4. The ratio between  $\Delta\varepsilon_{\alpha}$  and  $\Delta\varepsilon_w$  as a function of the water content for confined solutions of PG-water (upper panel) and PGME-water (lower panel).

Fig. 5. Temperature dependence of the relaxation times obtained from the curve fitting procedure shown in Fig. 3. Relaxation times for the confined solutions of PG-water and PGME-water are shown in (a) and (b), respectively. Relaxation times of the  $\alpha$ ,  $w$ , fast relaxation (of PG-water) and slow relaxation (of PGME) are given by solid symbols and the crossover to a fast local water relaxation by open symbols (i.e. for PGME-water in Fig. 5(b)). The VFT equation (Eq. 2) is used to describe the temperature dependences of the  $\alpha$ -relaxation and the slow relaxation (of PGME-water), whereas the temperature dependences of  $w$  and the fastest relaxation process is described by the Arrhenius equation (Eq. 3).

Fig. 6. Comparisons with corresponding bulk data. (a) and (b) show how the glass transition temperature,  $T_g$ , (which in the case of the confined solutions was estimated as the temperature where the  $\alpha$ -relaxation time extrapolates to 100 s), changes with composition in both bulk and confined solutions of PG and PGME, respectively. The temperature dependences of the  $\alpha$ -relaxation of the solutions confined in MCM-41 (solid symbols) are compared with corresponding bulk data (open symbols) in (c) and (d) for solutions of PG and PGME, respectively. The temperature dependences of the relaxation times in confinement and bulk are given by solid and dashed lines, respectively. The relaxation times of the  $w$ -relaxation in confinement (solid symbols) and bulk (open symbols) are shown in (e) and (f) for solutions of PG and PGME, respectively. Bulk data have been taken from Ref. 34.

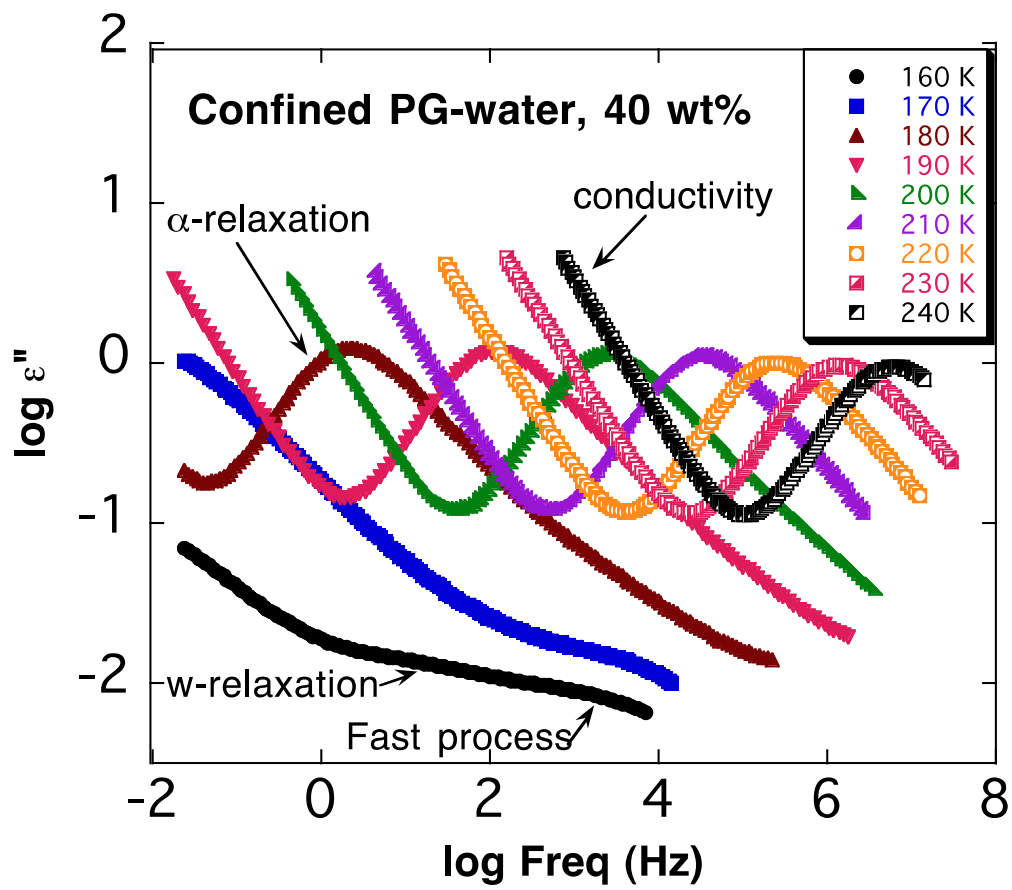


Fig. 1

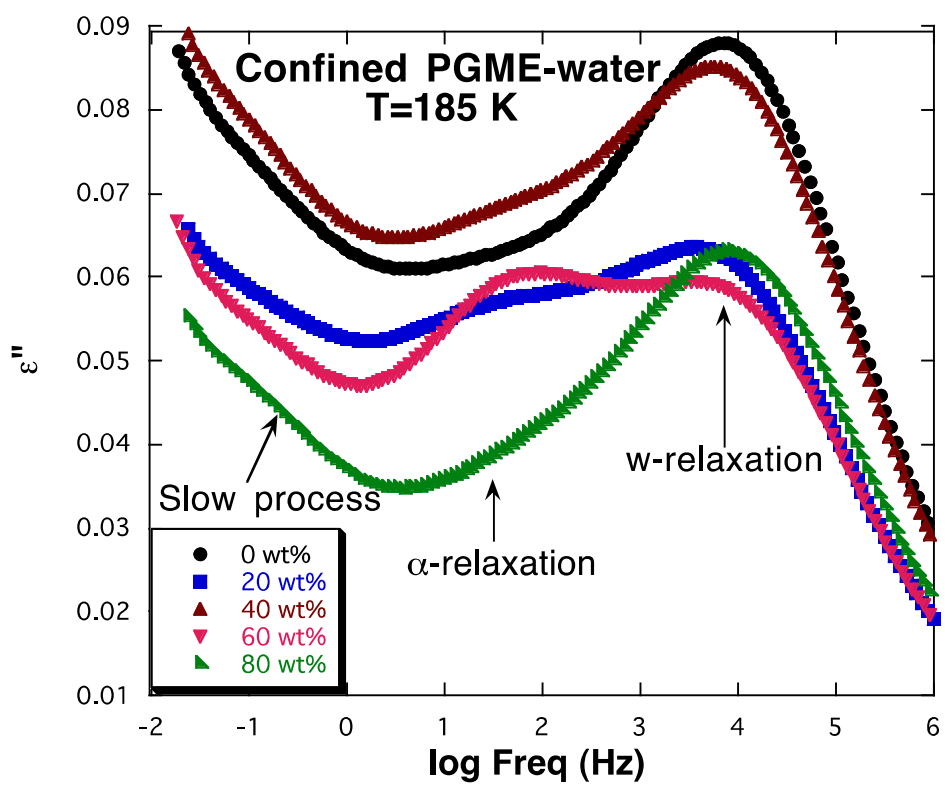


Fig. 2

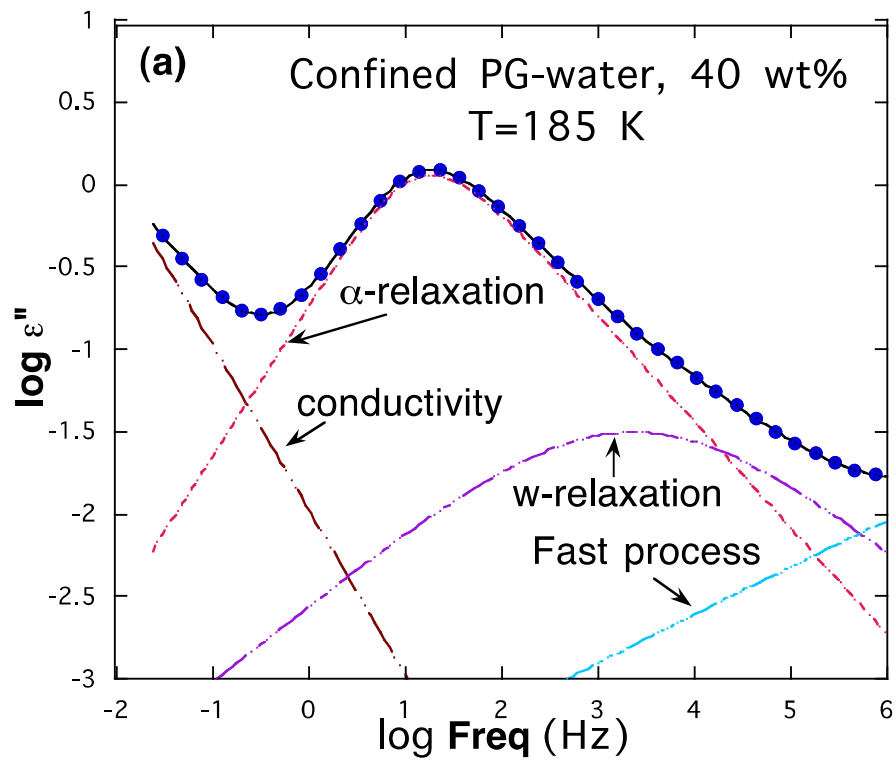


Fig. 3 (a)

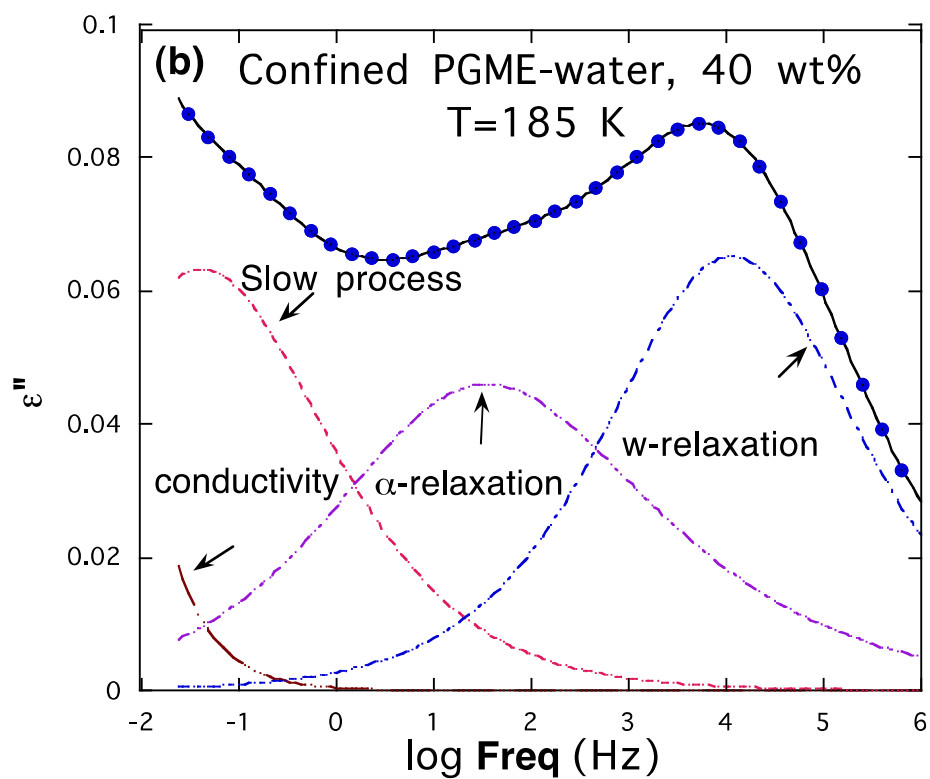


Fig. 3 (b)

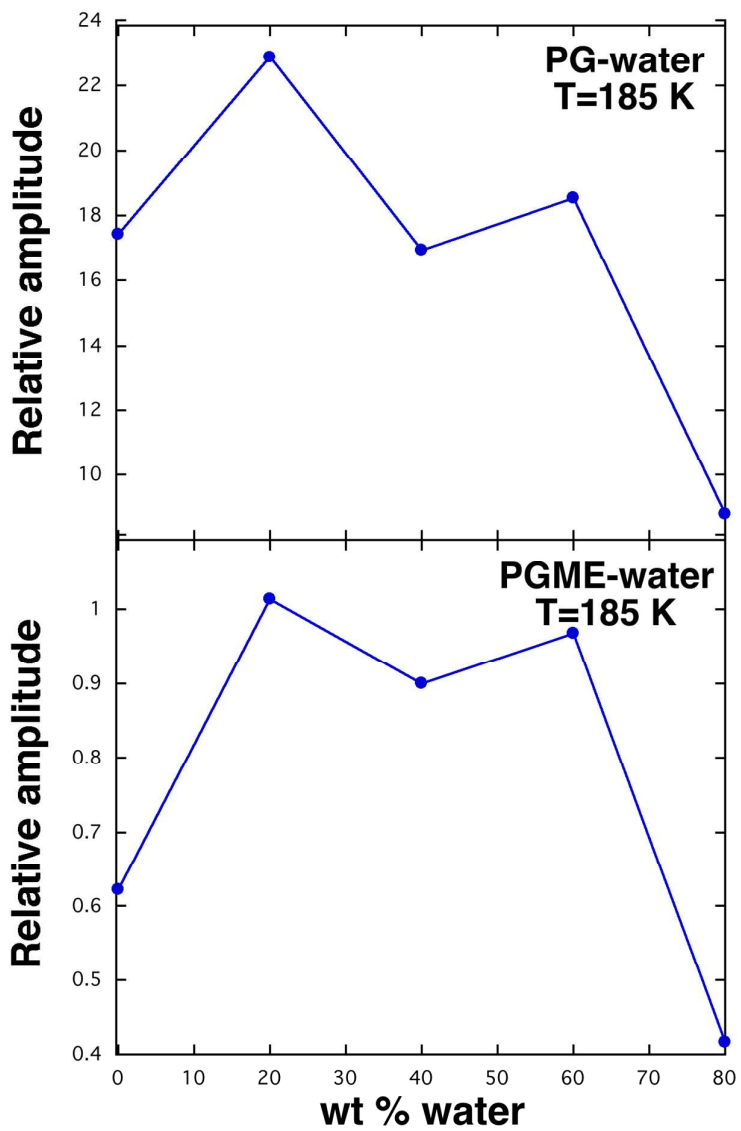


Fig. 4

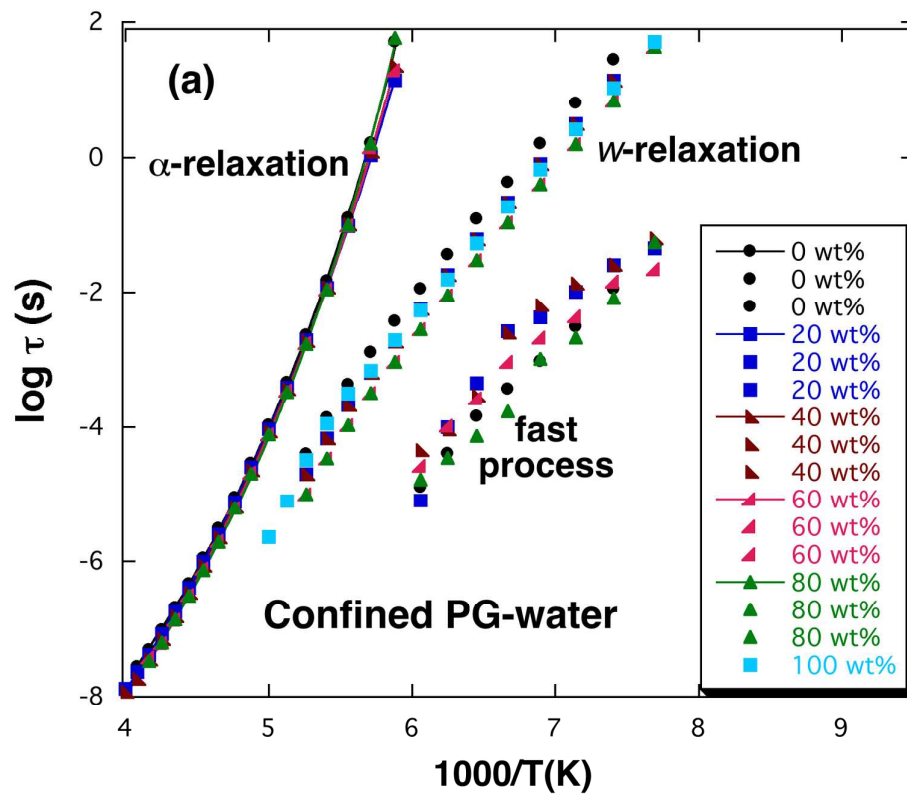


Fig. 5 (a)

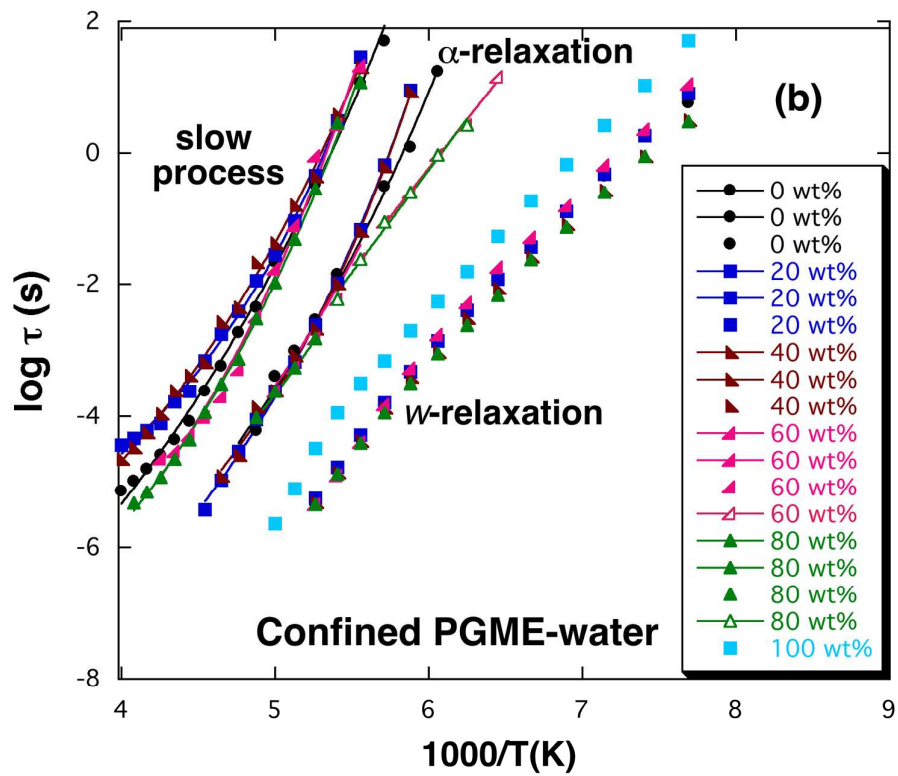


Fig. 5 (b)

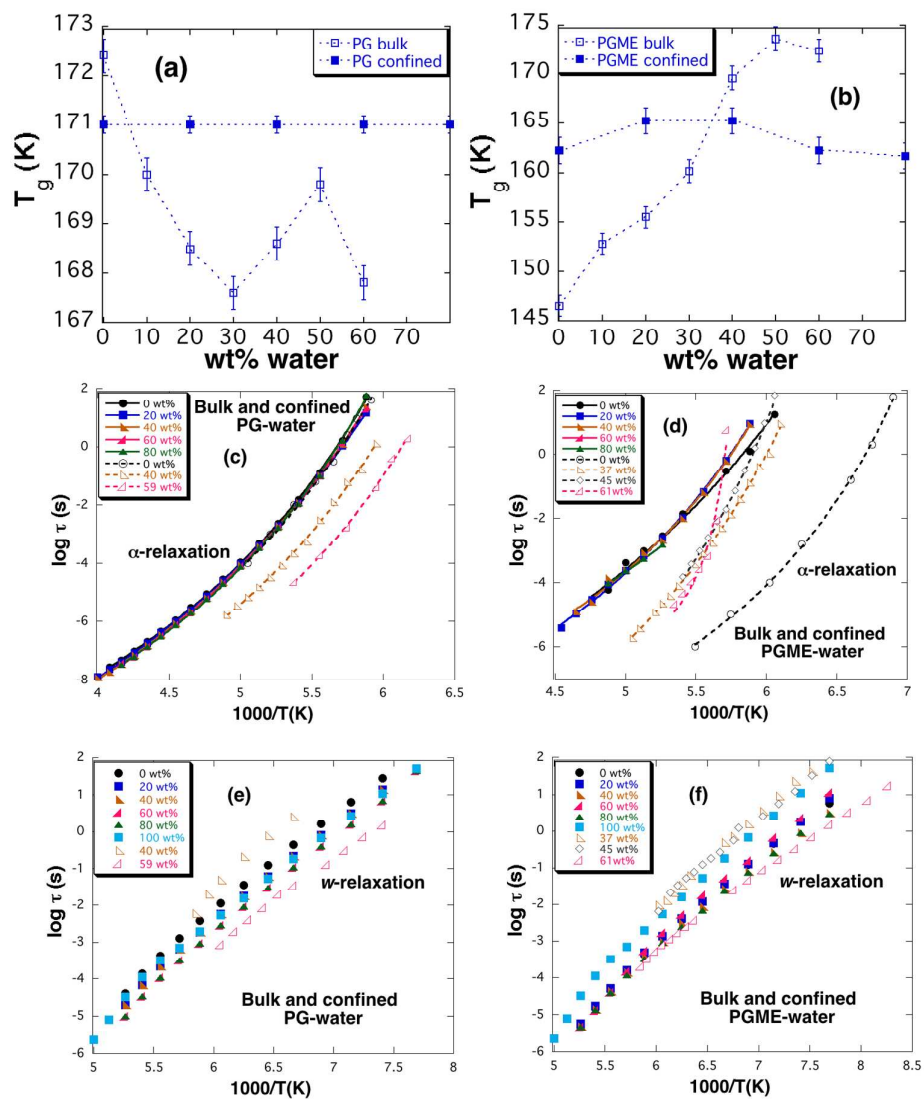


Fig. 6

## Tables

Table 1: Shape parameters for the two slowest relaxation processes, as obtained from the fitting procedure shown in Fig. 3. The temperature dependences of their relaxation times were described by the Vogel-Fulcher-Tammann (VFT) function<sup>49-51</sup> (Eq. 2), and these fit parameters are also shown together with the temperature where the relaxation time extrapolates to 100 s, corresponding to the glass transition temperature in the case of a  $\alpha$ -relaxation.

Sample	Relaxation process	$\tau_0$ (s)	Shape parameter $b$	Shape parameter $a$	Fragility D	$T_0$	$T$ ( $\tau=100$ s) K
0 wt% water PG-water	$\alpha$	$10^{-14}$	$0.65\pm 0.05$	$0.92\pm 0.05$	17	115	169
20 wt% water PG-water	$\alpha$	$10^{-15}$	$0.65\pm 0.05$	$0.91\pm 0.03$	23	106	168
40 wt% water PG-water	$\alpha$	$10^{-15}$	$0.65\pm 0.05$	$0.87\pm 0.07$	21	109	168
60 wt% water PG-water	$\alpha$	$10^{-15}$	$0.65\pm 0.05$	$0.85\pm 0.06$	21	109	167
80 wt% water PG-water	$\alpha$	$10^{-14}$	$0.65\pm 0.05$	$0.75\pm 0.09$	15	119	169
0 wt% water PGME-water	$\alpha$	$10^{-12}$	$0.65\pm 0.05$	$0.44\pm 0.01$	20	101	164
	slow	$10^{-12}$	1	$0.45\pm 0.02$	23	102	175
20 wt% water PGME-water	$\alpha$	$10^{-12}$	$0.65\pm 0.05$	$0.45\pm 0.02$	14	116	165
	slow	$10^{-9}$	1	$0.43\pm 0.02$	8	133	175
40 wt% water PGME-water	$\alpha$	$10^{-11}$	$0.65\pm 0.05$	$0.41\pm 0.05$	10	123	164
	slow	$10^{-10}$	1	$0.45\pm 0.02$	15	114	178
60 wt% water PGME-water	$\alpha$	$10^{-11}$	$0.65\pm 0.05$	$0.48\pm 0.04$	12	114	160
	slow	$10^{-12}$	1	$0.45\pm 0.02$	15	122	177
80 wt% water PGME-water	$\alpha$	$10^{-11}$	$0.65\pm 0.05$	$0.45\pm 0.05$	14	106	156
	slow	$10^{-12}$	1	$0.45\pm 0.02$	15	120	174

Table 2:

The shape parameter  $a$  for the two fastest relaxation processes, as obtained from the fitting procedure shown in Fig. 3. The temperature dependences of their relaxation times were described by the Arrhenius equation (Eq. 3), and the resulting fit parameters are also given.

Sample	Relaxation process	$\tau_0$ (s)	Shape parameter $a$	$E_a$ (kJ/mol)
0 wt% water PG-water	w	$10^{-17}$	$0.31 \pm 0.04$	51.8
	fast	$10^{-17}$	$0.22 \pm 0.03$	41.5
20 wt% water PG-water	w	$10^{-17}$	$0.41 \pm 0.04$	52.2
	fast	$10^{-15}$	$0.32 \pm 0.03$	40.9
40 wt% water PG-water	w	$10^{-17}$	$0.44 \pm 0.05$	53.3
	fast	$10^{-20}$	$0.33 \pm 0.02$	41.3
60 wt% water PG-water	w	$10^{-18}$	$0.47 \pm 0.01$	53.4
	fast	$10^{-15}$	$0.34 \pm 0.02$	42.2
80 wt% water PG-water	w	$10^{-18}$	$0.44 \pm 0.03$	52.8
	fast	$10^{-17}$	$0.32 \pm 0.03$	41.4
0 wt% water PGME-water	w	$10^{-17}$	$0.40 \pm 0.07$	53.1
20 wt% water PGME-water	w	$10^{-17}$	$0.41 \pm 0.06$	51.6
40 wt% water PGME-water	w	$10^{-17}$	$0.44 \pm 0.05$	52.4
60 wt% water PGME-water	w	$10^{-17}$	$0.45 \pm 0.04$	51.9
80 wt% water PGME-water	w	$10^{-17}$	$0.46 \pm 0.02$	52.7
100 wt% water	w	$10^{-17}$	$0.47 \pm 0.06$	53.3

**Abstract figure:** A typical fit of dielectric loss data (left) and glass transition temperatures of confined and bulk solutions of PG and PGME.

